

# Multi-Mirror Array Calculations With Optical Error

J. Goettsche<sup>1</sup>, S. Alexopoulos<sup>1</sup>, A. Dümmler<sup>1</sup>, S. K. Maddineni<sup>2</sup>

<sup>1</sup>FH Aachen, Solar-Institut Jülich, Heinrich-Mußmann-Str. 5, D-52428 Jülich

<sup>2</sup>FH Aachen

Corresponding author: goettsche@sj.fh-aachen.de

## Abstract

The optical performance of a 2-axis solar concentrator was simulated with the COMSOL Multiphysics® software. The concentrator consists of a mirror array, which was created using the application builder. The mirror facets are preconfigured to form a focal point. During tracking all mirrors are moved simultaneously in a coupled mode by 2 motors in two axes, in order to keep the system in focus with the moving sun. Optical errors on each reflecting surface were implemented in combination with the solar angular cone of  $\pm 4.65$  mrad.

As a result, the intercept factor of solar radiation that is available to the receiver was calculated as a function of the transversal and longitudinal angles of incidence. In addition, the intensity distribution on the receiver plane was calculated as a function of the incidence angles.

**Keywords:** solar process heat, concentrating collector, raytracing, point-focussing system

## Introduction

As part of the Germano-Hellenic bilateral research project SCoSCo an innovative collector concept was developed with the objective to design and test a concentrating collector that could be easily integrated in buildings; therefore, a concentrating solar collector with fixed mirror was found to be an interesting approach. Within the scope of the project in order to reduce costs, a concentrating collector with a simple flat-plate receiver is proposed (see Fig. 1). This is a novel concept that was not yet discussed in the context of solar process heat collectors [Weis2008]. The optical concentrator consists of an array of mirror facets placed in a box that protects the mirrors from wind loads and dirt [Sauerborn2008]. The innovative micro mirror box system has a built-in tracking mechanism, but the whole system is fixed.



**Fig. 1:** Mirror-Box Concentrator with Receiver

## Raytracing Setup

In order to optimize the optical setup, raytracing calculations were carried out using the COMSOL Multiphysics ray optics module. The COMSOL application builder was used to create and orient each facet of the mirror array such that the mirror normals were pointing at a half angle between the module normal and the receiver centre as seen from each facet centre. For non-normal incidence, all mirror facets were tilted by the same angles around the x and y axes. This is a deviation from the ideal situation in which each facet's orientation is adjusted individually but represents the real-world implementation in which it is possible to adjust the unit with only two drives.

In order to manage variations of the mirror array, two functions ('createFMSC' and 'RemoveMirrors') were programmed. If a different configuration is to be tested, first all existing mirrors have to be removed before the new set can be implemented and built.

The full set-up consists of the mirror array, the receiver box, the ray emitting surface and a plane below the mirror array that was used to count and display the rays that pass between the mirrors (see Fig. 2).

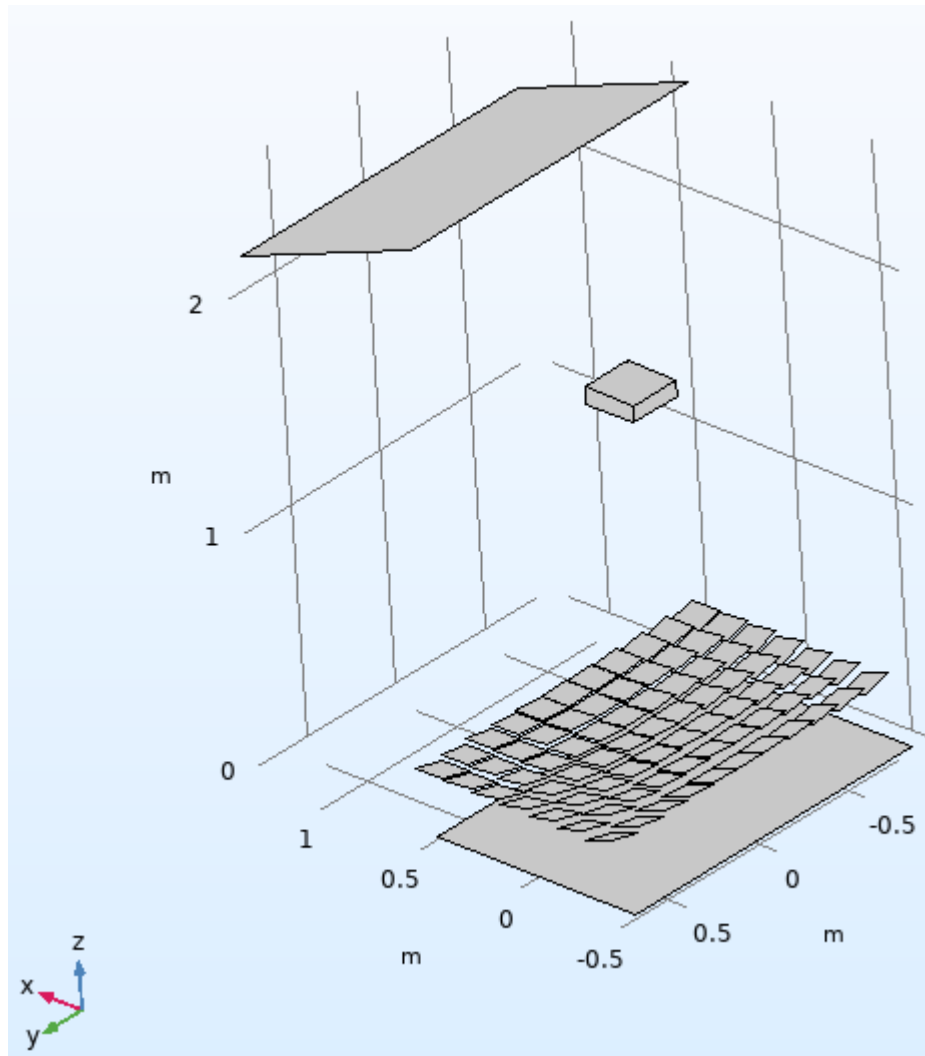


**Fig. 2:** Visualisation of the setup (7 x 11 mirrors) in COMSOL

The major results of the analysis were the intercept factor  $\gamma$ , defined as the fraction of beams that hit the absorber, and the expected intensity distribution  $I_{\text{abs}}(x,y;\theta_{\text{trans}},\theta_{\text{long}})$  on the absorber surface as a function of the angle of incidence as defined by the two angles  $\theta_{\text{trans}}$  and  $\theta_{\text{long}}$ , the angular projections of the incident beam on the (x,z) and (y,z) planes, respectively. The parameter variation included the number and size of mirrors, the gap between mirrors, the absorber size, the focal distance (equal to the distance between the array centre and the absorber centre), and the optical error.

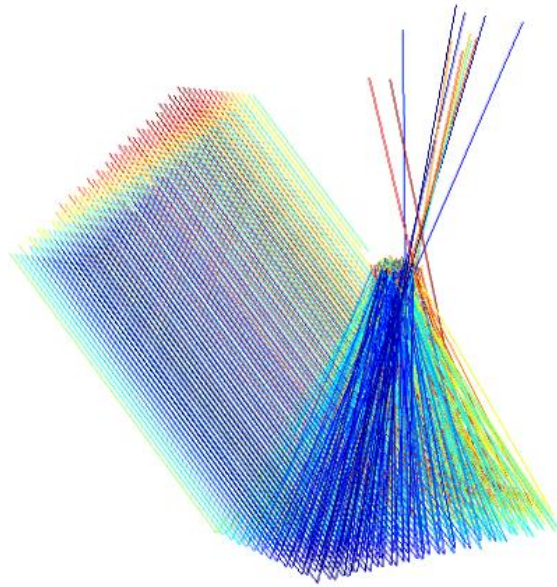


**Fig. 3:** View of the ray trajectories of the mirror-box system (300 rays)

The optical error was implemented on the mirror surface together with the angular distribution caused by the sun disk. This was done by modifying the equations of the reflection at the mirror surface (Wall 1 in Fig. 4).

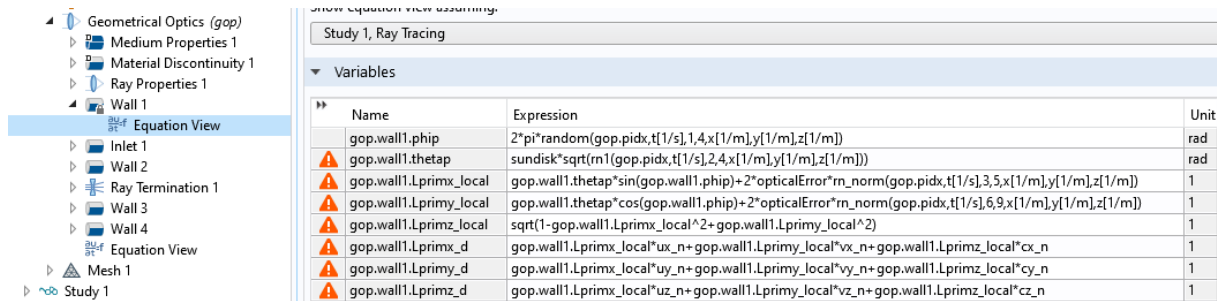


**Fig. 4:** Equation View of modified reflection condition

At the mirror surface the reflected rays are emitted in a cone with an opening angle that is determined by two random functions. The first random function creates a circular uniform random distribution that represents the sun disk (amplitude  $\pm 4.65$  mrad) while the second normal random function represents misalignments of the mirror surface that may occur due to multiple reasons. The random functions were tested with a single 1 mm x 1 mm mirror and an absorber at 10 m distance (see Fig. 5).

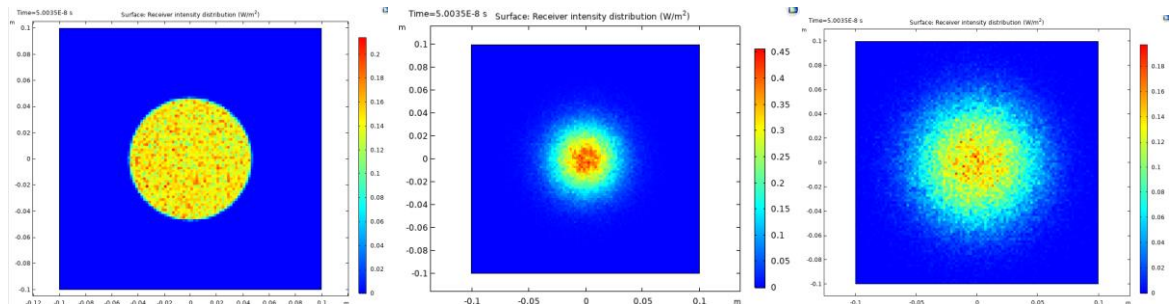


**Fig. 5:** Test of random functions (left: uniform sun disk effect, centre: normal distribution of other optical errors:  $\pm 1$  mrad, right: superposition of both effects), all images based on 100,000 rays

The sun disk effect is implemented on the mirror surfaces and not at the ray emitting surface because in this way, all emitted rays hit exactly the mirror array aperture area (except those that are shadowed by the receiver), which facilitates the calculation of the intercept factor.

## Results

Based on practical considerations and some parameter variations the following parameter set (Table 1) was found to be a good choice.

**Table 1:** Near-optimal parameter configuration

Receiver size	Mirror facets	Concentration factor	Focal length	Optical error	Intercept (100,000 rays)
20 cm x 20 cm	14 cm x 14 cm 7 x 11, gap: 1 mm	38.2	1.4 m	7 mrad	88.3 %

The resulting intensity distribution on the receiver and at the array background are displayed in Fig. 6. Due to the gaps between the mirrors 5.6 % of radiation is lost. It can be derived that almost all (93.5 % (=88.3/(100-5.6))) rays that are reflected by the mirrors actually hit the receiver. It is observed that the gap losses decrease when the focal length is increased and when the angle of incidence increases.

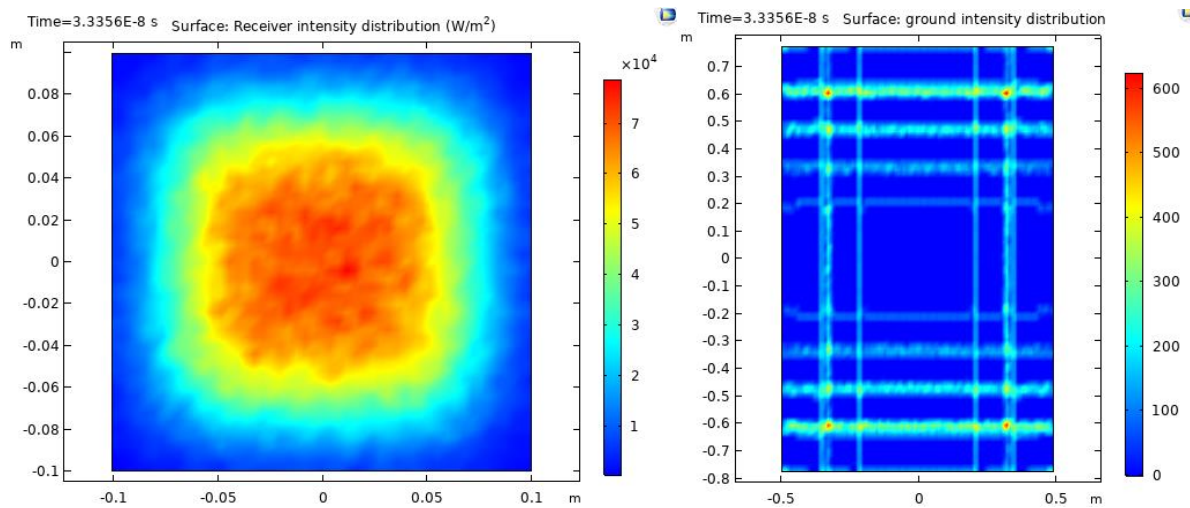


**Fig. 6:** Intensity distribution on receiver (left) and array background (right) of the configuration of Table 1 at 0° incidence, 300,000 rays

The intercept factor results of case of Table 1 at varying angles of incidence are shown in Table 2. This information is used by the thermal collector model calculations that were carried out using the Matlab/Simulink toolbox CARNOT [CARNOT 7.0]. Thereby the intercept factor at 0° incidence is implemented in the optical efficiency and the respective deviations at larger angles of incidence are taken into account by the so-called incidence angle modifier (IAM), which is defined as  $IAM(\theta) = \gamma(\theta)/\gamma(0)$ . IAM values for combinations of  $\theta_{trans}$  and  $\theta_{long}$  are calculated by the simplifying assumption that  $IAM(\theta_{trans}, \theta_{long}) = IAM(\theta_{trans}) \cdot IAM(\theta_{long})$ .

**Table 2:** Intercept data and derived IAM values from COMSOL simulations of the case of Table 1, left: transversal, right longitudinal variation of incidence angle (100,000 rays).

$\theta_{trans}$	$\gamma$ ( $\theta_{long} = 0$ )	IAM ( $\theta_{long} = 0$ )	$\theta_{long}$	$\gamma$ ( $\theta_{trans} = 0$ )	IAM ( $\theta_{trans} = 0$ )
0	0.883	1.0000	0	0.883	1.0000
15	0.887	1.0045	15	0.898	1.0169
30	0.886	1.0033	30	0.926	1.0484
45	0.795	0.9008	45	0.916	1.0374
60	0.653	0.7392	60	0.836	0.9466
75	0.482	0.5457	75	0.698	0.7900

It is further observed that the centre of the intensity distribution shifts with increasing angles of incidence (see Fig. 7). This effect is assigned to the astigmatism, which is caused by the coupled movement of the mirror facets. The optical losses caused by this shift can be compensated by a modification of the angle set point in the control system.

The details of this correction will be calculated based on centre-of-mass calculations of the receiver intensity distribution.

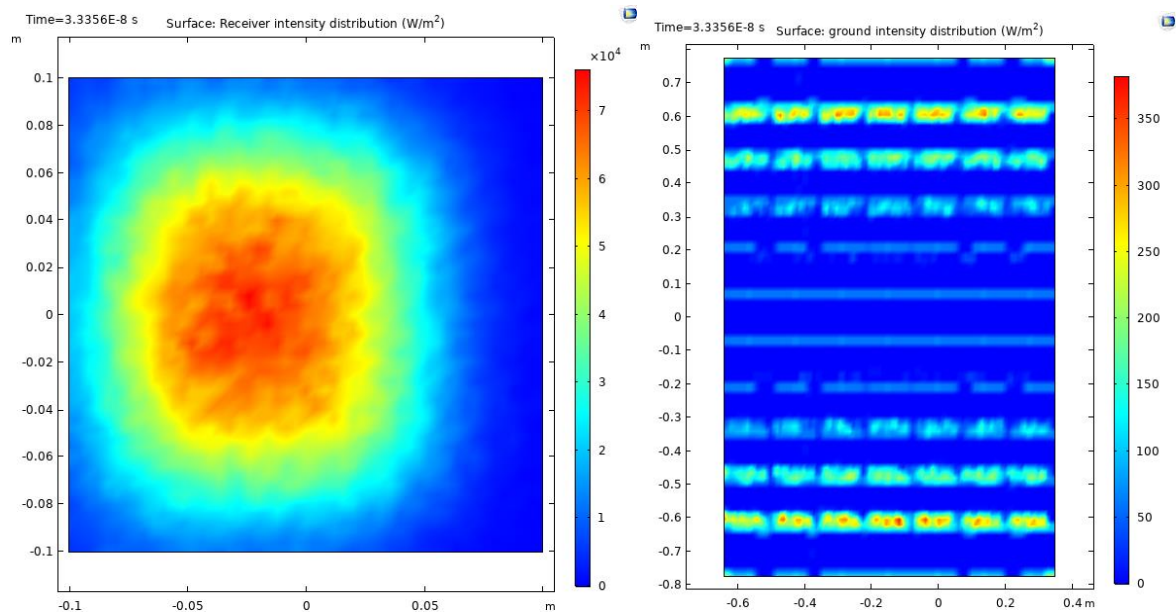


**Fig. 7:** Intensity distribution on receiver (left) and array background (right) of the configuration of Table 1 at  $\theta_{\text{trans}} = 30^\circ$ , 300,000 rays

When combinations of incidence angles are applied, in addition to the shift there is a rotation of the intensity distribution (Fig. 8).

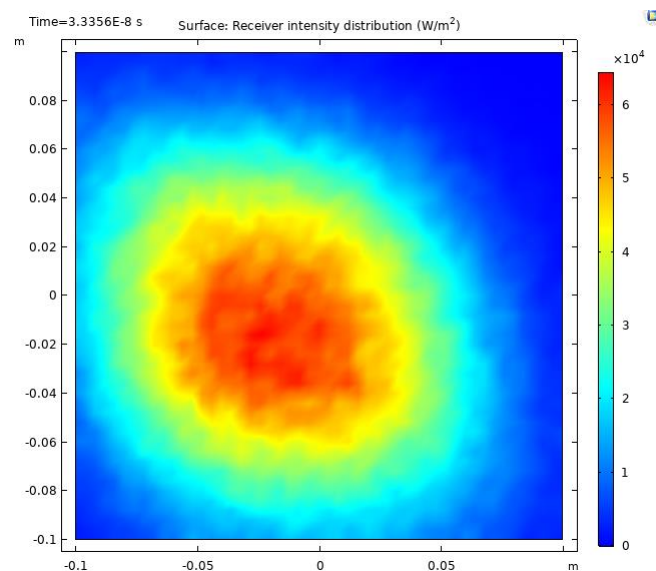


**Fig. 8:** Intensity distribution on receiver of the configuration of Table 1 at  $\theta_{\text{trans}} = 30^\circ$ ,  $\theta_{\text{long}} = 40^\circ$ , 300,000 rays

## Conclusion

Raytracing simulations were performed with respect to a novel concentrating solar collector design. The results confirm the feasibility of a coupled movement of the mirror facets using only two mechanical drives without unacceptable optical losses. Good results can be obtained even when optical errors of  $\pm 7$  mrad are present. Furthermore, the raytracing simulation results will help to optimize the mirror array control algorithms that shall take the observed shift of the intensity distribution into account.

## References

CARNOT Toolbox Ver. 7.0 for MATLAB/Simulink R2018b, Solar-Institut Juelich.

Sauerborn, M., Göttsche, J., Hoffschmidt, B., Schmitz, S., Rebholz, C., Ifland, D., Ansorge, F., Buck, R., Teufel, E., 2008. Test of a Mini-Mirror Array for Solar Concentrating Systems, EUROSUN 2008, Lisbon, Portugal.

Weiss, W., Rommel, M., 2008. Process heat collectors. State of the Art within Task 33. International Energy Agency.

### **Acknowledgements**

This project was co-funded by the German Federal Ministry of Education and Research and the Hellenic Secretariat for Research and Technology (SCOSCO project) in the framework of the Greek-German co-operation.